Spontaneous Ca^{2+} transients in rat pulmonary vein cardiomyocytes are increased in frequency and become more synchronous following electrical stimulation

Alasdair D. Henry[1], MacQuaide, N.[2], Burton, F.L.[2], Rankin, A.C.[2], Rowan, E.G.[1], Drummond R.M[1].

[1]Strathclyde Institute of Pharmacy and Biomedical Sciences, University of Strathclyde, Glasgow, UK

[2]Institute of Cardiovascular and Medical Sciences, College of Medical, Veterinary and Life Sciences, University of Glasgow, UK

Correspondence

robert.drummond@strath.ac.uk

Strathclyde Institute of Pharmacy and Biomedical Sciences

161 Cathedral Street

Glasgow, G4 0RE

+44(0)141 548 2027

Abstract

The pulmonary veins have an external sleeve of cardiomyocytes that are a widely recognised source of ectopic electrical activity that can lead to atrial fibrillation. Although the mechanisms behind this activity are currently unknown, changes in intracellular calcium (Ca^{2+}) signalling are purported to play a role. Therefore, the intracellular Ca^{2+} concentration was monitored in the pulmonary vein using fluo-4 and epifluorescence microscopy. Electrical field stimulation evoked a synchronous rise in Ca^{2+} in neighbouring cardiomyocytes; asynchronous spontaneous Ca^{2+} transients between electrical stimuli were also present. Immediately following termination of electrical field stimulation at 3 Hz or greater, the frequency of the spontaneous Ca^{2+} transients was increased from 0.45 ± 0.06 Hz under basal conditions to between 0.59 ± 0.05 and 0.65 ± 0.06 Hz ($P<0.001$). Increasing the extracellular Ca^{2+} concentration enhanced this effect, with the frequency of spontaneous Ca^{2+} transients increasing from 0.45 ± 0.05 Hz to between 0.75 ± 0.06 and 0.94 ± 0.09 Hz after electrical stimulation at 3 to 9 Hz ($P<0.001$), and this was accompanied by a significant increase in the velocity of Ca^{2+} transients that manifested as waves. Moreover, in the presence of high extracellular Ca^{2+}, the spontaneous Ca^{2+} transients occurred more synchronously in the initial few seconds following electrical stimulation. The ryanodine receptors, which are the source of spontaneous Ca^{2+} transients in pulmonary vein cardiomyocytes, were found to be arranged in a striated pattern in the cell interior, as well as along the periphery of cell. Furthermore, labelling the sarcolemma with di-4-ANEPPS showed that over 90% of pulmonary vein cardiomyocytes possessed T-tubules. These findings demonstrate that the frequency of spontaneous Ca^{2+} transients in the rat pulmonary vein are increased following higher rates of electrical stimulation and increasing the extracellular Ca^{2+} concentration.

Key words: pulmonary vein; pulmonary vein cardiomyocytes; atrial fibrillation; Ca^{2+} imaging; fluorescence microscopy; intracellular Ca^{2+} signalling; excitation-contraction coupling; membrane structure, ryanodine receptors; L-type Ca^{2+} channels; immunocytochemistry

Abbreviations:

EFS - Electrical field stimulation

FOV - Field of view

LTCC - L-type Ca^{2+} channel

NCX - Na^{+}/Ca^{2+} exchanger

PSS - Physiological salt solution

SR - Sarcoplasmic reticulum

ROI - Region of interest

RyR - Ryanodine receptor

1. Introduction

The pulmonary veins are widely accepted to play a significant role in the development of atrial fibrillation [1, 2]; however the underlying pathophysiology is still incompletely understood. A potential mechanism that may contribute to this arrhythmia is ectopic electrical activity originating in the cardiomyocytes that form a sleeve surrounding the blood vessel, which then propagates to the atria and disrupts normal sinus rhythm [3]. Independent electrical activity within the pulmonary vein was first demonstrated by Cheung in 1981, when spontaneous action potentials were recorded from cardiomyocytes in the pulmonary vein [4]. Nevertheless, subsequent studies have shown that there is significant variability in the incidence of spontaneous electrical activity, both within [5-8] and between [9] different species.

There is increasing evidence that Calcium (Ca^{2+}) release from the sarcoplasmic reticulum (SR) via the ryanodine receptor (RyR) plays an important role in the generation of ectopic electrical activity originating in the pulmonary vein. Low concentrations of ryanodine (0.5-2 μM), which would increase the opening probability of the RyRs, were shown to cause depolarisation of the cardiomyocyte resting membrane potential, and subsequent short trains of high frequency electrical stimuli triggered bursts of spontaneous action potentials that eventually self-terminated [6]. In contrast, spontaneous action potentials could not be induced by pacing the atrium in the presence of ryanodine, indicating that there are fundamental differences between cardiomyocytes in the pulmonary vein and atrium [6]. High concentrations of ryanodine (10 μM), sufficient to inhibit the RyR, have been shown to completely suppress triggered firing in the pulmonary vein, which was initiated by autonomic nerve stimulation [10], and further support for the involvement of the RyR was provided by the finding that the RyR stabilizer, K201 reduced the frequency of spontaneous action

potentials occurring in cardiomyocytes that were isolated from the pulmonary vein [11]. The link between intracellular Ca^{2+} and a change in the cardiomyocyte membrane potential is thought to be through the activation of the Na^{+}/Ca^{2+} exchanger (NCX), since inhibition of the exchanger has been found to suppress spontaneous electrical activity in pulmonary vein cardiomyocytes [5, 12-14].

We have previously shown that the cardiomyocytes in the rat pulmonary vein display spontaneous Ca^{2+} transients that often manifest as waves occurring asynchronously in neighbouring cells [15, 16], and a similar observation has recently been made regarding the mouse pulmonary vein [17]. A high concentration of ryanodine (20 μM) abolished the spontaneous Ca^{2+} transients in the majority of cardiomyocytes in the rat pulmonary vein [15], which is consistent with the notion that Ca^{2+} waves occur due to summation of the elementary Ca^{2+} sparks that result when Ca^{2+} is released from the SR [18]. Since spontaneous SR Ca^{2+} release typically occurs as a wave in the pulmonary vein cardiomyocytes, this will lead to a relatively slow increase in the activation of Ca^{2+}-activated currents as well as the NCX [19]. Indeed, it has been shown in isolated pulmonary vein cardiomyocytes that there is a noradrenaline induced inward current, which correlated with the size of the cytosolic Ca^{2+} transient during diastole [20]. Within the tissue, neighbouring cells will act as a current sink, diminishing any change in membrane potential that would occur through activation of the NCX [21]. Thus, these factors are likely to limit the ability of such asynchronous Ca^{2+} events to initiate spontaneous action potentials.

A direct mechanistic link between spontaneous Ca^{2+} transients and arrhythmogenic activity has previously been demonstrated in ventricular tissue. Electrical pacing (2 Hz) in the presence of isoproterenol and low extracellular K^{+} induced an increase in the frequency of

spontaneous Ca^{2+} transients after termination of stimulation, and this was accompanied by delayed after depolarisations (DADs) [22]. In another study on the ventricle, mathematical modelling showed that spontaneous Ca^{2+} transients occurred more synchronously after a period of high-frequency electrical stimulation (5 Hz), and that the spontaneous Ca^{2+} transient synchronicity correlated with the size of the resultant DADs [23]. Thus, it is apparent that for spontaneous Ca^{2+} transients to generate arrhythmogenic activity they must be entrained to occur more synchronously.

An important component of ectopic activity originating in the pulmonary vein is SR Ca^{2+} release via the RyR. Therefore, the aim of the present study was to investigate whether increasing cellular Ca^{2+} loading by raising the extracellular Ca^{2+} concentration ($[Ca^{2+}]_o$), in combination with brief periods of electrical stimulation, could synchronise the spontaneous Ca^{2+} transients and increase their potential arrhythmogenicity. The localisation of the RyRs and voltage-gated L-type Ca^{2+} channels (LTCCs) was also studied to provide further insight into how excitation-contraction coupling is controlled in pulmonary vein cardiomyocytes. Elucidating how intracellular Ca^{2+} signalling is regulated in the pulmonary vein is key towards understanding the causes of ectopic activity that can lead to atrial arrhythmias.

2. Materials and Methods

2.1. Animals and pulmonary vein isolation

Adult male Sprague-Dawley rats, weighing 250-430 g, were euthanised by cervical dislocation according to Schedule 1 of the Animals (Scientific Procedures) Act, 1986. After opening the thoracic cavity, the heart and lungs were quickly removed *en bloc* and placed in ice cold physiological salt solution (PSS) of the following composition (in mM); 119 NaCl, 25 $NaHCO_3$, 4.7 KCl, 1.17 $MgSO_4$, 1.18 KH_2PO_3, 2.5 $CaCl_2$ and 5.5 glucose (pH 7.4 with

95% O_2 and 5% CO_2). The main pulmonary vein branches to the left and posterior right lung lobes were micro-dissected and cleaned of any surrounding parenchyma under a Nikon SMZ645 stereomicroscope, which resulted in two separate pulmonary vein branches, measuring approximately 10-15 mm in length and 2-3 mm in outside diameter.

2.2. Imaging intracellular Ca^{2+}

The pulmonary vein was incubated for 60 min in the dark at room temperature, in PSS containing 10 μM fluo-4 AM and cremophor EL (0.03% v/v). The tissue was then washed and pinned onto a Sylgard® coated tissue chamber containing 4 ml PSS. The preparation was allowed 15 min for equilibration before any recording was performed. All experiments were carried out at room temperature (21-24 °C).

The pulmonary vein was imaged by wide-field epifluorescence microscopy, using an upright Zeiss Axioscop 50 epifluorescence microscope (Carl Zeiss, Germany) and a 40x objective lens (Achroplan, Carl Zeiss, Germany). Fluo-4 was excited by light from a 50 W mercury short ARC lamp (Osram, Germany), passed through a 450-490 nm band pass excitation filter. The emitted fluorescence was passed through a 515 nm long pass emission filter and images were captured using a Hamamatsu multiformat CCD camera (C4880-80, Hamamatsu Photonics K. K., Japan). Images were acquired with an exposure time of 109 ms (~9 frames per second) using WinFluor V3.2.19 (Dr. John Dempster, University of Strathclyde).

2.3. Electrical stimulation of the pulmonary vein

The pulmonary vein was stimulated by electrical field stimulation (EFS) using two platinum electrodes, positioned either side of the vein, approximately 1 cm apart. Rectangular pulses (2 ms duration) were applied at supramaximal voltage (80-100 V) using a Grass SD9 stimulator (Grass Instrument Co., USA).

2.5. Analysis of Ca^{2+} transients

Spontaneous Ca^{2+} transients were analysed for their peak amplitude and frequency using a custom-built plugin written for ImageJ. A region of interest (ROI) (20 x 20 pixels; equivalent to 5 x 5 μm) was selected in a cardiomyocyte and an initial record of pixel intensity over time was obtained. The plugin then fitted a polynomial 4^{th} order curved baseline, and divided the raw data by the calculated baseline value at each time-point to correct for photobleaching. The plugin contained an algorithm that distinguished peaks and nadirs in the data where there was a general increase or decrease in the fluorescence signal, and the amplitude ($\Delta F/F_{min}$) was automatically calculated for each Ca^{2+} transient. For the spontaneous Ca^{2+} transients, the mean amplitude during the recording period was calculated for each ROI, and the number of peaks per second was also obtained for the frequency (Hz). The velocity of the spontaneous Ca^{2+} waves was measured as distance/time using the "Kymograph" plugin for ImageJ.

The synchronisation of spontaneous Ca^{2+} transients was analysed using a script written in the Python language. A mask was applied from a maximum projection image to isolate a region of tissue displaying spontaneous Ca^{2+} transients. The code then determined the minimum and maximum intensity of each pixel throughout an image series and then calculated the half maximal pixel intensity for every pixel. A threshold of 50% was applied in order to create a binary image series that distinguished pixels with a higher or lower intensity than the

threshold, and the fraction of pixels with a higher intensity than the threshold was calculated for each frame providing a synchronisation index between 0 and 1 for the whole image series. For example, during an electrically evoked response all the pixels comprising the tissue would display an increase in fluorescence simultaneously and the maximum synchronisation index would be 1. However, during the spontaneous activity, not all pixels will show a simultaneous increase in fluorescence and the fraction that does, therefore provides a measure of the synchronisation index. Once the synchronisation index was calculated for each frame over time, the maximum synchronisation index was taken as the highest value recorded during the first 2 s post-EFS, and the last 2 s of the image series.

2.6. Experimental protocols

2.6.1. Effect of increasing the extracellular Ca^{2+} concentration on the electrically evoked Ca^{2+} transients

The pulmonary vein was electrically stimulated at 1 Hz and an initial control recording of the electrically evoked Ca^{2+} transients was obtained. The concentration of Ca^{2+} in the PSS was increased from 2.5 to 4.5 mM, and the response to EFS was re-examined after a 2 min equilibration period.

3.6.2. Effect of a period of electrical stimulation on the subsequent spontaneous Ca^{2+} transients

The tissue was electrically stimulated at 1 Hz for 5 s, and the fluo-4 fluorescence was recorded immediately after termination of the stimulus. Following a 2 min rest period, the pulmonary vein was electrically stimulated at 3 Hz for 5 s, and another recording was made. The same procedure was repeated to examine the effect of EFS at 5, 7 and 9 Hz on the subsequent spontaneous activity.

2.7. Cardiomyocyte isolation

Cardiomyocytes were isolated from the pulmonary vein using a modified Langendorff perfusion protocol. Initially, the system was primed with Ca^{2+} free Tyrode's solution of the following composition (in mM); 120 NaCl, 20 HEPES, 5.4 KCl, 0.52 NaH_2PO_4, 3.5 $MgCl_2$, 20 taurine, 10 creatine, 11.1 glucose (pH 7.4 with NaOH). This Tyrode's solution also contained 1 mM EGTA to chelate any residual Ca^{2+}, and the temperature was maintained at 37 °C. Rats were anesthetised with sodium pentobarbital (Euthanase®) (100 mg/kg) and euthanised by cervical dislocation, before the heart and lungs were removed and placed in Ca^{2+} free Tyrode's solution containing 0.2 ml Heparin (5000 U/ml). The heart, with the lungs still attached, was retrogradely perfused through the aorta to clear blood from the coronary and pulmonary circulation, before being digested with 0.66 mg/ml (240 U/ml) collagenase type I (Worthington Biochemical Corporation) and 0.04 mg/ml protease type XIV (Sigma Aldrich) for approximately 10 min. The heart and lungs were then perfused with Ca^{2+} free Tyrode's solution containing 0.8% w/v BSA for 7 min to block any further enzymatic activity. The ventricles and left atria were separated and the cardiomyocytes were dissociated in Kraft brühe (KB) solution of the following composition (in mM); 70 L-glutamic acid, 25

KCl, 20 taurine, 10 KH_2PO_4, 3 $MgCl_2$, 10 glucose, 10 HEPES, 0.5 EGTA, 0.8 % BSA; pH 7.4 with KOH), by gently triturating diced chunks with a plastic Pasteur or fire polished glass pipette respectively. Cardiomyocytes were obtained from both the left and right ventricle. The pulmonary veins were dissected from the lungs and digested for a further 20 min at 37 °C in collagenase type I (20 mg/ml) and protease type XIV (10 mg/ml). The pulmonary veins were then diced into small chunks and triturated in KB solution using a fire polished glass pipette. Isolated cardiomyocytes were stored at 4 °C until use.

2.8. Immunocytochemistry

Isolated cardiomyocytes were allowed to settle on 0.1% poly-L-lysine coated cover slips before being fixed with 2.5% w/v formalin (1% paraformaldehyde) for 20 min. The cardiomyocytes were then permeabilised with 0.1% Triton-X-100 for 15 min, and non-specific binding was blocked by 60 min exposure to 10% goat serum. The cover slips were exposed to 25 µl diluted primary antibody overnight at 4 °C. Rabbit polyclonal $Ca_v1.2$ (1:100) (Merck Millipore, Billerica, MA, USA) was used to detect the LTCCs and mouse (IG1) monoclonal RyR2 (1:50) (Pearce Antibody Products, Thermo Fisher Inc., Waltham, MA, USA) was used for the RyRs. Thereafter, the cells were incubated for 60 min at room temperature with the appropriate secondary antibodies (goat anti-mouse or goat anti-rabbit IgG H+L), conjugated with Alexa Fluor® 488 (2 mg/ml, dissolved in PBS at a dilution factor of 1:250) (Invitrogen™, Glasgow, UK). Phosphate buffered saline (PBS) of the following composition (in mM); 10 Na_2HPO_4, 2.7 KCl and 137 NaCl (pH 7.4) was used to wash the cells between steps. The cover slips were mounted face down on glass slides with 25 µl hard set Vectashield® containing 4',6-diamidino-2-phenylindole (DAPI) and stored in the dark at 4 °C before imaging.

Immunolabelled cardiomyocytes were imaged by confocal microscopy (Leica TCS SP5, Leica Microsystems, UK) with a Leica (HCX PL APO CS; NA 1.4) 63x lens. This yielded a pixel size of 0.141 μm x 0.141 μm. Sampling along the z-direction during optical-sectioning was 0.54 μm. The cells were excited at 488 nm and the fluorescence emission was captured at 510 nm. At each frame, DAPI was excited at 360 nm and the emission was captured at 460 nm. Leica image file format (LIF) files were imported into ImageJ for analysis and presentation using LOCI Bio-Formats Importer software.

2.9. Imaging the sarcolemma

Isolated cardiomyocytes were maintained in PSS containing 1 mM $CaCl_2$ and a drop of the cell suspension was placed on a glass cover slip. The sarcolemma was imaged by confocal microscopy after adding 1 μM di-4-ANEPPS as described above for Alexa Fluor® 488. When imaging the intact pulmonary vein, 10 μM di-4-ANEPPS was added to the PSS and the vein was imaged by epifluorescence microscopy. Cardiomyocytes were considered to possess T-tubules if they had elements of a similar fluorescence to the surface membrane protruding transversely from the surface or in the interior of the cells.

2.10. Chemicals and drugs

Fluo-4 AM and di-4-ANEPPS (both Invitrogen™, Life Technologies, Glasgow, UK) were prepared in DMSO at stock concentrations of 1 and 2 mM, and stored at -20 and 4 °C respectively. Bovine serum albumin, creatine, EGTA (ethylene glycol-bis(2-aminoethylether)-N,N,N′,N′-tetraacetic acid), formalin, goat serum, HEPES (4-(2-hydroxyethyl)-1-piperazineethanesulfonic acid), L-glutamate, PBS, poly-L-lysine, taurine and Triton X-100 were all obtained from Sigma Aldrich (Gillingham, Dorset, UK). Heparin was obtained from Leo Laboratories Ltd. (Hurley, Berkshire, UK). Vectashield® was obtained from Vector

Laboratories (Peterborough, Cambridgeshire, UK), and stored in the dark at 4 °C. All other reagents were from VWR (Lutterworth, Leicestershire, UK).

2.11. Statistical analysis

Data are expressed as the mean ± standard error of the mean (s.e.m.). Cardiomyocyte dimensions were compared via a one-way analysis of variance (ANOVA) with Tukey's post-test. The amplitude of the electrically evoked, and the frequency of the spontaneous Ca^{2+} transients, before and after increasing the $[Ca^{2+}]_o$, were compared using Student's paired *t*-tests. The frequency, amplitude, wave velocity and synchronisation following EFS at increasing frequencies were compared to the control group (no prior EFS) using a repeated-measures ANOVA followed by Dunnett's multiple comparison test. Statistical significance was considered when $P<0.05$.

3. Results

3.1. Pulmonary vein cardiomyocytes

Wide-field fluorescence imaging of the di-4-ANEPPS loaded pulmonary vein showed rod shaped cardiomyocytes were present in the extrapulmonary regions and smaller intrapulmonary branches of the vein. The cardiomyocytes tended to be orientated in an oblique manner in relation to the longitudinal axis of the vein (Figure 1A), although occasionally they were arranged in a more circular manner, as has been previously reported [24]. Enzymatic dissociation of the cardiomyocytes in the pulmonary vein revealed that 92% of the cells had a network of transverse (T) – tubules, typically running perpendicular to the longitudinal axis of the cell, and there was a mean distance of 1.86 ± 0.03 μm between the striations (n = 36). However, the degree of tubulation was variable between cardiomyocytes (Figure 1B). Ventricular cardiomyocytes had a dense T-tubule system, with T-tubules

projecting across the horizontal axis of the cell, whereas T-tubules were not observed in atrial cardiomyocytes (Figure 1B). The length of the pulmonary vein cardiomyocytes was 135.7 ± 5.06 μm and they had a width of 23.63 ± 1.10 μm (n = 28), which was significantly larger than left atrial cardiomyocytes, which were 99.77 ± 4.54 μm long (n = 17, $P<0.001$) and 17.17 ± 1.25 μm wide (n = 17, $P<0.05$). Ventricular cardiomyocytes were not significantly different in length compared to those of the pulmonary vein, being 142.1 ± 5.94 μm long; however, they were significantly wider at 40.6 ± 2.13 μm (n = 22, $P<0.001$) (Figure 1C).

3.2. Localisation of the L-type Ca^{2+} channels and ryanodine receptors

Influx of Ca^{2+} through the LTCCs is important for the generation of electrically evoked Ca^{2+} transients in the pulmonary vein [15]. Therefore, their localisation was examined in isolated cardiomyocytes using antibodies raised against the $Ca_V1.2$ subunit [25]. Pulmonary vein cardiomyocytes displayed a punctate distribution of LTCCs in the interior and along the periphery of the cells. However, there was evidence of striations in 83% of the cardiomyocytes studied, where they were spaced 1.72 ± 0.11 μm apart (n = 6 cells from 5 separate isolations) (Figure 2A). The localisation of the RyRs was also determined by immunostaining for the cardiac isoform, RyR2 [26], where it was found that they were predominantly arranged in regular transverse striations, spaced 1.70 ± 0.05 μm apart along the length of the cells. However, RyRs were also present along the periphery of the cell and this was observed in every cardiomyocyte studied (n = 7 cells from 5 separate isolations) (Figure 2B).

3.3. Electrically evoked Ca^{2+} transients in the pulmonary vein

When intracellular Ca^{2+} was monitored in the pulmonary vein using fluo-4, EFS evoked a synchronous rise in Ca^{2+} in neighbouring cardiomyocytes (Figure 3A and supplementary

movie 1). Electrically evoked Ca^{2+} transients often occurred in discrete regions of the tissue that were surrounded by cardiomyocytes that appeared to be unresponsive to stimulation. The synchronous nature of the electrically evoked Ca^{2+} transients within a group of neighbouring cells is illustrated in the pseudo-linescan image, which shows a simultaneous rise in Ca^{2+} in all of the cardiomyocytes across the linescan during each electrical stimulus (Figure 3B). Asynchronous spontaneous Ca^{2+} transients, occurring between the electrically evoked Ca^{2+} transients, were also evident in the ROI analysis for individual cardiomyocytes. Furthermore, the cardiomyocytes still responded with a Ca^{2+} transient, regardless of whether or not spontaneous Ca^{2+} transients were present between those that were evoked (Figure 3C).

The effect of increasing $[Ca^{2+}]_o$ on the electrically evoked Ca^{2+} transients was then investigated. Representative recordings in Figure 4 show the fluo-4 fluorescence in the FOV during EFS at 1 Hz in two pulmonary veins from different rats (Figures 4A and B). In 22% of preparations studied, there appeared to be an increase in the fluorescence signal that preceded each electrically evoked Ca^{2+} transient (Figure 4B and C). To determine the effect of increasing the $[Ca^{2+}]_o$ on the spontaneous Ca^{2+} transients that occurred between the electrical stimuli, further ROI analysis was carried out at the level of individual cardiomyocytes. Figure 5A displays the fluo-4 fluorescence between electrical stimuli (top panel) and during an electrical pulse (bottom panel), when the $[Ca^{2+}]_o$ was 2.5 mM (left panels) and 4.5 mM (right panels). It was found that there was an approximately four-fold increase in the frequency of spontaneous Ca^{2+} transients between those that were electrically evoked from 0.11 ± 0.06 Hz to 0.41 ± 0.28 Hz (n = 16 cardiomyocytes from 7 PVs from 6 rats, $P<0.001$) (Figure 5C and D). An increase in the frequency of spontaneous Ca^{2+} transients was observed in the majority of tissues studied (6/7) and not just in those that displayed an increase in fluorescence in the FOV, as shown in Figure 4B. Moreover, in approximately half of the cardiomyocytes,

spontaneous Ca^{2+} transients were not observed between electrical stimuli until after the extracellular Ca^{2+} concentration was increased.

3.4. Effect of a period of electrical stimulation on the subsequent spontaneous Ca^{2+} transients

To further explore the relationship between EFS and spontaneous Ca^{2+} transients in the pulmonary vein, brief periods of EFS were applied at increasing frequencies in order to determine if the spontaneous Ca^{2+} transients would occur more synchronously upon cessation of the stimulus. After a period of EFS at 1 Hz, the frequency of spontaneous Ca^{2+} transients was not significantly different from the control recordings without prior EFS. However, after a period of EFS at 3 Hz, the frequency of spontaneous Ca^{2+} transients was increased by 31 ± 11% ($P<0.001$ *vs.* no prior EFS). The frequency of spontaneous Ca^{2+} transients was increased by 44 ± 11% after EFS at 5 Hz; however, there was no further increase after EFS at 7 Hz or 9 Hz (Figure 6A and B). Despite EFS causing an increase in the frequency of the spontaneous Ca^{2+} transients, there was no significant difference in their amplitude compared to the control recordings without any prior EFS (n = 26 cardiomyocytes from 6 PVs from 6 rats, n.s.) (Figure. 6A and C). The mean velocity of the spontaneous Ca^{2+} waves was also largely unaffected by a period of EFS at 1-9 Hz (n = 21 cardiomyocytes from 7 PVs from 7 rats).

When $[Ca^{2+}]_o$ was increased, it was notable that there was a much greater increase in the frequency of the spontaneous transients following cessation of a period of EFS, compared to what was observed with standard PSS. The frequency of spontaneous Ca^{2+} transients increased by 92 ± 15% immediately after a period of EFS at 3 Hz ($P<0.001$ *vs*. no prior EFS), and by 133 ± 17% after EFS at 5 Hz ($P<0.001$ *vs*. no prior EFS). No further increase in the frequency of spontaneous Ca^{2+} transients occurred after EFS at 7 or 9 Hz (Figure 6A and B,

online movies 2 and 3). Again, the amplitude of the spontaneous Ca^{2+} transients was not significantly changed after a period of EFS up to 5 Hz. However, there was a significant reduction in the Ca^{2+} transient amplitude after EFS at 7 and 9 Hz, by 14 ± 7% and 21 ± 7% respectively (n = 34 cardiomyocytes from 6 PVs from 6 rats, P<0.001 *vs*. no prior EFS) (Figure 6A and C). In contrast to the findings in standard PSS, where the wave velocity was essentially unchanged following EFS, the wave velocity was increased by 38 ± 8% after a period of EFS at 3 Hz (P<0.05 *vs*. no prior EFS). There was an increase of 65 ± 10% after EFS at 5 Hz, after which the wave velocity plateaued at the higher frequencies of stimulation (32 cardiomyocytes from 6 PVs from 6 rats, P<0.001 *vs*. no prior EFS) (Figure 6 A and D).

Following the observation that raised $[Ca^{2+}]_o$ caused a significant increase in the frequency of the spontaneous Ca^{2+} transients after EFS, we were interested in determining whether this equated to a greater degree of synchronisation of these events in neighbouring cells. To this end, the fraction of pixels displaying a rise in fluorescence was determined for each time point. In standard PSS, the maximum synchronisation index during the first 2 s of the recordings was 0.24 ± 0.04 with no prior EFS, and this was unchanged after a period of EFS at 1 Hz. There was a non-significant increase in the maximum synchronisation index after EFS at 3 Hz and above. During the last 2 s of the recordings the peak synchronisation index after a period of EFS at 1-9 Hz was no different than without prior EFS (n = 6 PVs from 6 rats, n.s.) (Figure 7 A and B).

Following raised $[Ca^{2+}]_o$, the maximum synchronisation index was 0.17 ±0.02 without prior EFS, and was 0.28 ± 0.04 and 0.44 ±0.05 during the first 2 s after EFS at 1 and 3 Hz; however neither increase was statistically significant. The maximum synchronisation index was significantly increased after EFS at 5 and 7 Hz, being 0.70 ± 0.12 and 0.62 ± 0.13

respectively (P<0.01 *vs.* no prior EFS), and was also significantly greater after a period of EFS at 9 Hz (P<0.05 *vs.* no prior EFS). The synchronisation index increased immediately after a period of EFS, but declined again before the end of the recording period. Thus, during the last 2 s of the recordings, the peak synchronisation index was not significantly changed from 0.19 ± 0.02 after a period of EFS at 1-9 Hz (Figure 7A and C).

4. Discussion

In the present study, we observed that more than 90% of cardiomyocytes in the pulmonary vein possessed T-tubules. While the degree of tubulation was variable between cardiomyocytes, they were spaced approximately 2 μm apart. T-tubules have been observed in pulmonary vein cardiomyocytes from the rat [20] and canine [27]; however, they appear to be absent in the mouse, where di-8-ANEPPS predominately stained the periphery of the cells [17]. It is noteworthy that rat pulmonary vein cardiomyocytes possessed organised T-tubules, as rat atrial cardiomyocytes are typically thought to have only a rudimentary T-tubule network [28-30], although more recent evidence showed a well organised T-tubule system in 10% of the cell population [31]. Studies in the rat and human suggest that T-tubule density in atrial cardiomyocytes is correlated with the cell width [29, 32]; therefore, the observation that pulmonary vein cardiomyocytes were significantly larger than those from the left atria could explain why an appreciable T-tubule network was observed in the majority of the pulmonary vein cardiomyocytes.

In pulmonary vein cardiomyocytes, RyRs had a striated arrangement, which is in agreement with previous studies in the rat [33] and mouse [17]. However, this study is the first to demonstrate that RyRs also have a junctional distribution along the periphery of pulmonary vein cardiomyocytes, similar to that observed in rat atrial cardiomyocytes [34, 35]. We have

previously shown that Ca^{2+} influx during depolarisation is dependent on activation of LTCCs [15]. Therefore, the observation that pulmonary vein cardiomyocytes have T-tubules and typically showed a striated distribution of LTCCs, suggests that there may be a greater degree of Ca^{2+} influx occurring in proximity to the RyRs in the cell interior during depolarisation. A recent study has shown that when rat pulmonary vein cardiomyocytes with more extensive T-tubules are electrically stimulated, they tended to display an initial rise in Ca^{2+} in the centre as well as at the periphery of the cell (W-shaped) [36]. On the other hand, in those cells that had a sparse T-tubule distribution, the initial rise in intracellular Ca^{2+} occurred only at the periphery of the cells (U-shaped) [36]. A potential function of T-tubules in pulmonary vein cardiomyocytes might therefore be to enable a more spatially homogeneous increase in intracellular Ca^{2+} upon depolarisation.

When intracellular Ca^{2+} signalling was monitored in the pulmonary vein using fluo-4, EFS evoked a synchronous rise in Ca^{2+} in neighbouring cardiomyocytes. Although it wasn't systematically investigated in the current study, it was apparent that some regions of the pulmonary vein did not respond to electrical stimulation. The reasons for this are unclear, although a previous electrophysiological study on the rat pulmonary vein showed that cardiomyocytes in a region that was distal to the left atrium did not respond to electrical pacing with action potentials, suggesting that there may be regional heterogeneity in the response of the pulmonary vein to EFS [37]. A recent study has shown that pulmonary veins that are densely tubulated are located is discrete groups, often surrounded by groups of cells that are sparsely tubulated [36]. Therefore, regional heterogeneity in the function of the pulmonary vein cardiomyocytes could be reflective of region variation in their ultrastructure.

During EFS at 1 Hz, when the pulmonary vein was maintained in standard PSS, spontaneous Ca^{2+} transients were often observed in the intervals between those that were electrically evoked. These spontaneous events were also asynchronous in neighbouring cells. This differs somewhat from what has been reported in the rat ventricle, where spontaneous Ca^{2+} transients were only observed between electrical stimuli after $[Ca^{2+}]_o$ was raised above 6 mM [38]. Spontaneous SR Ca^{2+} release is widely accepted to occur in cardiomyocytes when the concentration of Ca^{2+} in the SR is above a critical threshold [39-41]. Therefore the propensity for the pulmonary vein to display spontaneous Ca^{2+} transients under normal conditions could be explained by these cardiomyocytes already having a high degree of SR loading. Rat atrial cardiomyocytes have been shown to have a greater Ca^{2+} buffering capacity, due to an increased rate of SR reuptake, and thus were found to have greater SR Ca^{2+} concentrations compared with ventricular cardiomyocytes [42]. Furthermore, atrial cardiomyocytes have been shown to have higher SERCA expression levels, compared to ventricular cardiomyocytes in several species [43], including human [44], where SERCA mRNA expression was also greater and phospholamban expression lower. The relative expression of SR proteins therefore warrants future investigation in pulmonary vein cardiomyocytes. Certainly, the Ca^{2+} handling properties fit into the paradigm that an innate property of pulmonary vein cardiomyocytes that they are very efficient at sequestering cytosolic Ca^{2+}.

After increasing $[Ca^{2+}]_o$, there was an increased frequency of spontaneous Ca^{2+} transients occurring between those that were electrically evoked, and in some preparations there appeared to be a global increase in fluorescence that preceded the electrically evoked response. The relationship between EFS and spontaneous Ca^{2+} transients was therefore further explored, where it was found that after cessation of a period of EFS at 3 Hz or greater, spontaneous Ca^{2+} transients occurred at an increased frequency, and this effect was enhanced

after increasing $[Ca^{2+}]_o$. This is very similar to the findings in rat ventricular tissue that the frequency of spontaneous Ca^{2+} transients was increased after EFS at 1 Hz, and then further increased after EFS and 2 and 3 Hz [38], and in another study the frequency of spontaneous Ca^{2+} transients was found to be greater following a period of stimulation at 5 Hz compared to 2 Hz, particularly in the presence of high $[Ca^{2+}]_o$ [23].

The spontaneous Ca^{2+} transients that occurred after cessation of EFS at 3 Hz or above appeared to be present in multiple cardiomyocytes at the same time, suggesting increased synchronisation of SR Ca^{2+} release in neighbouring cells. In the presence of high $[Ca^{2+}]_o$, after cessation of EFS at 5 Hz or greater, there was a transient increase in the synchronisation of the spontaneous Ca^{2+} transients, which lasted for a few seconds, before returning to control levels by the end of the recording period. Of particular note is the finding that in half of the pulmonary veins that were studied, the synchronisation index reached as high as 0.93-0.97. It was previously shown in rat ventricle that immediately after cessation of a period of EFS in the presence of isoproterenol and low extracellular K^+, spontaneous Ca^{2+} transients emerged simultaneously in neighbouring cardiomyocytes and caused DADs [22]. Therefore, it is tempting to speculate that similar findings might be made in the pulmonary vein under the present conditions.

The relationship between spontaneous SR Ca^{2+} release and SR content has been shown to be highly non-linear in cardiomyocytes, becoming exponential in the range in which spontaneous Ca^{2+} transients are observed [45, 46]. Due to the steepness of this relationship, when spontaneous Ca^{2+} transients are already present, any increase in SR Ca^{2+} release will occur due to increased transmembrane Ca^{2+} flux, rather than prolonged changes in SR content [45, 46]. Two possible explanations for the increase in the frequency of the spontaneous Ca^{2+}

transients are therefore; increased sensitisation of the RyRs [47] or increased SERCA activity [48]. For instance, Ca^{2+}/calmodulin dependent protein kinase II (CaMKII), which is known to phosphorylate RyRs and increase SR Ca^{2+} release [49], has been shown to be activated in ventricular cardiomyocytes by electrical pacing at 2 Hz or higher [50]. The frequency and velocity of Ca^{2+} waves has also been shown to be modulated by CaMKII through its effect on SERCA activity [51]. In the present study, after increasing $[Ca^{2+}]_o$, the velocity of Ca^{2+} waves was considerably increased after a period of EFS at 3 Hz or greater. It is believed that the velocity of Ca^{2+} waves is dependent on the rate of Ca^{2+} uptake at the wave front through SERCA, which primes the RyRs for activation by cytosolic Ca^{2+} as the wave propagates along the cell [48, 52, 53]. Therefore, the increase in the frequency and velocity of Ca^{2+} waves in the pulmonary vein cardiomyocytes could have been due to elevated SERCA activity, which would increase the rate at which the local SR Ca^{2+} content reaches the threshold for spontaneous release.

In summary, this study shows that the frequency of spontaneous Ca^{2+} transients in the rat pulmonary vein is highly sensitive to periods of EFS, becoming increased after EFS at the higher rates of stimulation, and this effect is enhanced after increasing $[Ca^{2+}]_o$. The aforementioned conditions resulted in a greater synchronisation of spontaneous Ca^{2+} transients during the first few seconds after cessation of EFS. These findings demonstrate important mechanisms that can synchronise spontaneous SR Ca^{2+} release and potentially underlie arrhythmogenic activity in pulmonary vein cardiomyocytes.

Acknowledgements and funding

The author(s) would like to acknowledge Dr John Dempster, whose software was used for the acquisition of the data presented within this paper. In addition they would like to thank Prof.

Godfrey Smith for his valuable thoughts on the results and Dr Craig Doherty for reading the manuscript. This work was funded by a British Heart Foundation studentship. The authors declare no potential conflicts of interest.

Author contributions

Study conception and design – ADH, ACR, EGR, RMD

Acquisition of data – ADH

Analysis and interpretation of data – ADH, NM, FLB, EGR, RMD

Drafting of manuscript – ADH, RMD

Critical revision - ADH, NM, FLB, RMD

References

[1] M. Haïssaguerre, J. Pierre, D.C. Shah, A. Takahashi, M. Hocini, G. Quiniou, S. Garrigue, A. Le Mouroux, P. Le Métayer, J. Clémenty, Spontaneous initiation of atrial fibrillation by ectopic beats originating in the pulmonary veins, N Engl J Med., 339 (1998) 659-666.

[2] S.-A. Chen, M.-H. Hsieh, C.-T. Tai, C.-F. Tsai, V.S. Prakash, W.-C. Yu, T.-L. Hsu, Y.-A. Ding, M.-S. Chang, Initiation of atrial fibrillation by ectopic beats originating from the pulmonary veins: electrophysiological characteristics, pharmacological responses, and effects of radiofrequency ablation., Circulation., 100(18) (1999) 1879-1886.

[3] M. Chard, R. Tabrizchi, The role of pulmonary veins in atrial fibrillation: A complex yet simple story, Pharmacol Ther., 124 (2009) 207-218.

[4] D.W. Cheung, Electrical activity of the pulmonary vein and its interaction with the right atrium in the guinea-pig, J Physiol., 314 (1981a) 445-456.

[5] Y.-J. Chen, S.-A. Chen, Y.-C. Chen, H.-I. Yeh, M.-S. Chang, C.-I. Lin, Electrophysiology of single cardiomyocytes isolated from rabbit pulmonary veins: implication in initiation of focal atrial fibrillation, Basic Res Cardiol., 97 (2002) 26-34.

[6] H. Honjo, M.R. Boyett, R. Niwa, S. Inada, M. Yamamoto, K. Mitsui, T. Horiuchi, N. Shibata, K. Kamiya, I. Kodama, Pacing-induced spontaneous activity in myocardial sleeves of pulmonary veins after treatment with ryanodine, Circulation., 107 (2003) 1937-1943.

[7] L.-W. Lo, Y.-C. Chen, Y.-J. Chen, W. Wongcharoen, C.-I. Lin, S.-A. Chen, Calmodulin kinase II inhibition prevents arrhythmic activity induced by alpha and beta adrenergic agonists in rabbit pulmonary veins, Eur J Pharmacol., 571 (2007) 197-208.

[8] C.-A. Seol, J. Kim, W.-T. Kim, J.-M. Ha, H. Choe, Y.-J. Jang, E.-B. Shim, J.-B. Youm, Y.-E. Earm, C.-H. Leem, Simulation of spontaneous action potentials of cardiomyocytes in pulmonary veins of rabbits., Prog Biophys Mol Biol., 96(1-3) (2008) 132-151.

[9] T.-M. Wang, C.-E. Chiang, J.-R. Sheu, C.-H. Tsou, H.-M. Chang, H.-N. Luk, Homogenous distribution of fast response action potentials in canine pulmonary vein sleeves: a contradictory report, Int J Cardiol, 89 (2003) 187-195.

[10] E. Patterson, S.S. Po, B.J. Scherlag, R. Lazzara, Triggered firing in pulmonary veins initiated by in vitro autonomic nerve stimulation, Heart Rhythm, 2 (2005) 624-631.

[11] Y.-J. Chen, Y.-C. Chen, W. Wongcharoen, C.-I. Lin, S.-A. Chen, Effect of K201, a novel antiarrhythmic drug on calcium handling and arrhythmogenic activity of pulmonary vein cardiomyocytes., B JPharmacol., 153(5) (2008) 915-925.

[12] P.-S. Chen, C.-C. Chou, A.-Y. Tan, S. Zhou, M.C. Fishbein, C. Hwang, H.S. Karagueuzian, S.-F. Lin, The mechanisms of atrial fibrillation., J Cardiovasc electrophysiol., 17(3) (2006) 2-7.

[13] E. Patterson, R. Lazzara, B. Szabo, H. Liu, D. Tang, Y.-H. Li, B.J. Scherlag, S.S. Po, Sodium-calcium exchange initiated by the Ca^{2+} transient: an arrhythmia trigger within pulmonary veins., J Am Coll Cardiol., 47(6) (2006) 1196-1206.

[14] I. Namekata, Y. Tsuneoka, A. Takahara, H. Shimada, T. Sugimoto, K. Takeda, M. Nagaharu, K. Shigenobu, T. Kawanishi, H. Tanaka, Involvement of the Na^+/Ca^{2+} exchanger in the automaticity of guinea-pig pulmonary vein myocardium as revealed by SEA0400, J Pharmacol Sci., 110 (2009) 111-116.

[15] S.J. Logantha, S.F. Cruickshank, E.G. Rowan, R.M. Drummond, Spontaneous and electrically evoked Ca^{2+} transients in cardiomyocytes of the rat pulmonary vein., Cell Calcium., 48 (2010) 150-160.

[16] S.F. Cruickshank, R.M. Drummond, The effects of hypoxia on $[Ca^{2+}]i$ signalling in phenotypically distinct myocytes from the rat pulmonary vein, Journal of Physiology, 548P (2003) P56.

[17] K. Rietdorf, M.D. Bootman, M.J. Sanderson, Spontaneous, pro-arrhythmic calcium signals disrupt electrical pacing in mouse pulmonary vein sleeve cells, PLoS One, 9(2) (2014) e88649.

[18] H. Cheng, M.R. Lederer, W.J. Lederer, M.B. Cannell, Calcium sparks and $[Ca^{2+}]i$ waves in cardiac myocytes., Am J Physiol., 270(1 pt. 1) (1996) 148-159.

[19] K. Schlotthauer, D.M. Bers, Sarcoplasmic reticulum Ca^{2+} release causes myocyte depolarization : underlying mechanism and threshold for triggered action potentials, Circ Res., 87 (2000) 774-780.

[20] Y. Okamoto, M. Takano, O. Takayoshi, K. Ono, Arrhythmogenic coupling between the Na^+ -Ca^{2+} exchanger and inositol 1,4,5-triphosphate receptor in rat pulmonary vein cardiomyocytes, J Mol Cell Cardiol., 52(5) (2012) 988-997.

[21] Y. Xie, D. Sato, A. Garfinkel, Z. Qu, J.N. Weiss, So little source, so much sink: requirements for afterdepolarizations to propagate in tissue., Biophys J., 99(5) (2010) 1408-1415.

[22] K. Fujiwara, H. Tanaka, H. Mani, T. Nakagami, T. Takamatsu, Burst emergence of intracellular Ca^{2+} waves evokes arrhythmogenic oscillatory depolarization via the Na^{+}-Ca^{2+} exchanger: simultaneous confocal recording of membrane potential and intracellular Ca^{2+} in the heart, Circ Res., 103(5) (2008).

[23] J.A. Wasserstrom, Y. Shiferaw, W. Chen, S. Ramakrishna, H. Patel, J.E. Kelly, M.J. O'Toole, A. Pappas, N. Chirayil, N. Bassi, L. Akintilo, M. Wu, R. Arora, G.L. Aistrup, Variability in timing of spontaneous calcium release in the intact rat heart is determined by the time course of sarcoplasmic reticulum calcium load / novelty and significance, Circ Res., 107 (2010) 1117-1126.

[24] H. Hashizume, M. Tango, T. Ushiki, Three-dimensional cytoarchitecture of rat pulmonary venous walls: a light and scanning electron microscopic study, Anatomy and Embryology, 198 (1998) 473-480.

[25] W.A. Catterall, E. Perez-Reyes, T. Snutch, J. Striessnig, International Union of Pharmacology. XLVIII. Nomenclature and structure-function relationships of voltage-gated calcium channels., Pharmacol Rev., 57(4) (2005) 411-425.

[26] K. Otsu, H.F. Willard, V.K. Khanna, F. Zorzato, N.M. Green, D.H. MacLennan, Molecular cloning of cDNA encoding the Ca^{2+} release channel (ryanodine receptor) of rabbit cardiac muscle sarcoplasmic reticulum., J Biol Chem., 265(23) (1990) 13462-13483.

[27] P. Melnyk, J.R. Ehrlich, M. Pourrier, L. Villeneuve, T.-J. Cha, S. Nattel, Comparison of ion channel distribution and expression in cardiomyocytes of canine pulmonary veins versus left atrium., Cardiovasc Res., 65(1) (2005) 104-116.

[28] F. Brette, K. Komukai, C.H. Orchard, Validation of formamide as a detubulation agent in isolated rat cardiac cells, American Journal of Physiology - Heart and Circulatory Physiology, 283 (2002) 1720-1728.

[29] M.M. Kirk, L.T. Izu, Y. Chen-Izu, S.L. McCulle, W.G. Wier, C.W. Balke, S.R. Shorofsky, Role of the transverse-axial tubule system in generating calcium sparks and calcium transients in rat atrial myocytes, J Physiol., 547(2) (2003) 441-451.

[30] I. Smyrnias, W. Mair, D. Harzheim, S.A. Walker, H.L. Roderick, M.D. Bootman, Comparison of the T-tubule system in adult rat ventricular and atrial myocytes, and its role in excitation-contraction coupling and inotropic stimulation, Cell Calcium., 47 (2010) 210-223.

[31] M. Frisk, J.T. Koivumäki, P.A. Norseng, M.M. Maleckar, O.M. Sejersted, W.E. Louch, Variable t-tubule organization and Ca^{2+} homeostasis across the atria., Am J Physiol Heart Circ Physiol., 307(4) (2014) 609-620.

[32] M.A. Richards, J.D. Clarke, P. Saravanan, N. Voigt, D. Dobrev, D.A. Eisner, A.W. Trafford, K.M. Dibb, Transverse tubules are a common feature in large mammalian atrial myocytes including human, Am J Physiol Heart Circ Physiol., 301 (2011) 1996-2005.

[33] Y. Xiao, X. Cai, A. Atkinson, S.J. Logantha, M. Boyett, H. Dobrzynski, Expression of connexin 43, ion channels and Ca^{2+}-handling proteins in rat pulmonary vein cardiomyocytes, Exp Ther Med., 12(5) (2016) 3233-3241.

[34] M.N. Schulson, D.R. Scriven, P. Fletcher, E.D. Moore, Couplons in rat atria form distinct subgroups defined by their molecular partners, J Cell Sci., 24(7) (2011) 1167-1174.

[35] L. Mackenzie, M.D. Bootman, M.J. Berridge, P. Lipp, Predetermined recruitment of calcium release sites underlies excitation-contraction coupling in rat atrial myocytes, J Physiol., 530(3) (2001) 417-429.

[36] C. Pasqualin, A. Yu, C.O. Malécot, F. Gannier, C. Cognard, D. Godin-Ribuot, J. Morand, P. Bredeloux, V. Maupoil, Structural heterogeneity of the rat pulmonary vein myocardium: consequences on intracellular calcium dynamics and arrhythmogenic potential., Sci Rep., 8(1) (2018).

[37] Y.V. Egorov, V.S. Kuz'min, A.V. Glukhov, L.V. Rosenshtraukh, Electrophysiological characteristics, rhythm, disturbances and conduction discontinuities under autonomic stimulation in the rat pulmonary vein myocardium, J Cardiovas Electrophysiol., 26(10) (2015) 1130-1139.

[38] T. Kaneko, H. Tanaka, M. Oyamada, S. Kawata, T. Takamatsu, Three distinct types of Ca(2+) waves in Langendorff-perfused rat heart revealed by real-time confocal microscopy., Circ Res., 86(10) (2000) 1093-1099.

[39] C.L. Overend, D.A. Eisner, S.C. O'Neill, The effect of tetracaine on spontaneous Ca^{2+} release and sarcoplasmic reticulum calcium content in rat ventricular myocytes., J Physiol., 502(3) (1997) 471-479.

[40] D. Jiang, B. Xiao, D. Yang, R. Wang, P. Choi, L. Zhang, H. Cheng, S.-R. Chen, RyR2 mutations linked to ventricular tachycardia and sudden death reduce the threshold for store-overload-induced Ca^{2+} release (SOICR). Proc Natl Acad Sci U S A., 101(35) (2004) 13062-13067.

[41] B. Xiao, X. Tian, W. Xie, P.P. Jones, S. Cai, X. Wang, D. Jiang, H. Kong, L. Zhang, K. Chen, M.P. Walsh, H. Cheng, S.R. Chen, Functional consequence of protein kinase A-dependent phosphorylation of the cardiac ryanodine receptor: sensitization of store overload-induced Ca^{2+} release., J Biol Chem., 282(41) (2007) 30256-30264.

[42] A.P. Walden, K.M. Dibb, A.W. Trafford, Differences in intracellular calcium homeostasis between atrial and ventricular myocytes., J Moll Cell Cardiol., 46(4) (2009) 463-473.

[43] I. Lüss, P. Boknik, L.R. Jones, U. Kirchhefer, J. Knapp, B. Linck, H. Lüss, A. Meissner, F.U. Müller, W. Schmitz, U. Vahlensieck, J. Neumann, Expression of cardiac calcium regulatory proteins in atrium v ventricle in different species., J Mol Cell Cardiol., 31(6) (1999) 1299-1314.

[44] P. Bokník, C. Unkel, U. Kirchhefer, U. Kleideiter, O. Klein-Wiele, J. Knapp, B. Linck, H. Lüss, F. Müller, W. Schmitz, U. Vahlensieck, N. Zimmermann, L. Jones, J. Neumann, Regional expression of phospholamban in the human heart., Cardiovasc Res., 43(1) (1999) 67-76.

[45] M.E. Díaz, A.W. Trafford, S.C. O'Neill, D.A. Eisner, Measurment of sarcoplasmic reticulum Ca^{2+} content and sarcolemmal Ca^{2+} fluxes in isolated rat ventricular myocytes during spontaneous Ca^{2+} release, J Pysiol., 501 (1997a) 3-16.

[46] T.R. Shannon, K.S. Ginsburg, D.M. Bers, Quantitative assessment of the SR Ca^{2+} leak-load relationship., Circ Res., 91(7) (2002) 594-600.

[47] L.A. Venetucci, A.W. Trafford, S.C. O'Neill, D.A. Eisner, The sarcoplasmic reticulum and arrhythmogenic calcium release., Cardiovasc Res., 77(2) (2008) 285-292.

[48] J.T. Maxwell , L.A. Blatter, Facilitation of cytosolic calcium wave propagation by local calcium uptake into the sarcoplasmic reticulum in cardiac myocytes., J Physiol., 590(23) (2012) 6037-6045.

[49] X.H. Wehrens, S.E. Lehnart, S.R. Reiken, A.R. Marks, Ca^{2+}/calmodulin-dependent protein kinase II phosphorylation regulates the cardiac ryanodine receptor, Circ Res., 94(6) (2004) 61-70.

[50] E. Dries, V. Bito, I. Lenaerts, G. Antoons, K.R. Sipido, N. Macquaide, Selective modulation of coupled ryanodine receptors during microdomain activation of calcium/calmodulin-dependent kinase II in the dyadic cleft., Circ Res., 113(11) (2013) 1242-1252.

[51] N. MacQuaide, J. Dempster, G.L. Smith, Measurement and modeling of Ca^{2+} waves in isolated rabbit ventricular cardiomyocytes, Biophys J., 93(7) (2007) 2581-2595.

[52] M. Keller, J.P. Kao, M. Egger, E. Niggli, Calcium waves driven by "sensitization" wave-fronts., Cardiovasc Res., 74(1) (2007) 39-45.

[53] M.K. Stokke, K. Hougen, I. Sjaastad, W.E. Louch, S.J. Briston, U.H. Enger, K.B. Andersson, G. Christensen, D.A. Eisner, O.M. Sejersted, A.W. Trafford, Reduced SERCA2 abundance decreases the propensity for Ca^{2+} wave development in ventricular myocytes, Cardiovasc Res., 86(1) (2010) 63-71.

Figure Legends

Figure 1. Morphology of rat pulmonary vein cardiomyocytes. **A.** An intact segment of the pulmonary vein, which has been labelled with di-4-ANEPPS and imaged using wide-field fluorescence microscopy with a 40x (left) and 63x (right) objective lens. **B.** An image, obtained at 40x, of the di-4-ANEPPS fluorescence in an isolated pulmonary vein cardiomyocyte imaged by confocal microscopy (PV). Boxes to the right display wide-field images of pulmonary vein cardiomyocytes, imaged at 63x (n = 36 cells from 3 separate isolations). An image, obtained at 40x of a left atrial and a ventricular cardiomyocyte are also presented (representative of n = 18 atrial and 16 ventricular cells from 3 isolations). **C.** Dimensions along the longitudinal (length) and transverse (width) axes of ventricular (V, n =22 cells from 13 independent cell isolations), left atrial (LA, n = 17 cells from 14 isolations) and pulmonary vein (PV, n = 28 cells, from 14 isolations) cardiomyocytes. $^{\#}P<0.05$, $^{***}P<0.001$, $^{\#\#\#}P<0.001$ and $^{‡‡‡}P<0.001$ determined by one-way ANOVA and Tukey's post-test. Scale bars represent 20 μm.

Figure 2. Localisation of LTCCs and RyRs in pulmonary vein cardiomyocytes. **A.** Isolated pulmonary vein cardiomyocyte labelled with a primary antibody against $Ca_V1.2$ (green). The image is representative of 10 cardiomyocytes from 5 independent cell isolations. **B.** Pulmonary vein cardiomyocyte labelled with a primary antibody against RyR2 (green). Image is representative of 7 cardiomyocytes from 5 isolations. Nuclei have been labelled with DAPI (blue). The regions in the orange rectangles have been expanded and the scale bars represent 20 μm. Fluorescence intensity profiles were obtained from the dashed lines indicated in the expanded images in A and B.

Figure 3. Electrically evoked Ca^{2+} transients in rat pulmonary vein. **A.** Sequential images (i-vi), obtained every 109 ms, of the fluo-4 fluorescence in the pulmonary vein during EFS. Images are presented using green pseudo-colour scale. Scale bar represents 20 μm. **B.** Pseudo-linescan image depicting the fluo-4 fluorescence over time in the section of tissue indicated by the white dashed line in panel (i). Arrow heads represent the electrical stimulus, which was applied at 1 Hz. **C.** The fluorescence intensity in the regions of interest (ROIs) indicated in panel (vi), together with the fluorescence in the entire field of view (FOV), are displayed over a 14 s recording period. Note the spontaneous Ca^{2+} transients in ROIs 1 and 2, indicated with asterisks. Images are representative of 16 PVs from 14 rats.

Figure 4. The effect of increasing the $[Ca^{2+}]_o$ on the electrically evoked Ca^{2+} transients in the rat pulmonary vein. **A.** Representative recording of the fluo-4 fluorescence in the entire FOV during EFS at 1 Hz, in a control recording and after $[Ca^{2+}]_o$ was increased from 2.5 to 4.5 mM. **B.** Representative fluo-4 images (scale bar = 20 μm) and FOV fluorescence recordings from a pulmonary vein from a different rat showing an increase in fluorescence that preceded each electrical stimulus. **C.** A section from each recording has been superimposed and presented using an expanded time-scale. Recordings and images are representative of 9 PVs from 7 rats.

Figure 5. The effect of increasing the $[Ca^{2+}]_o$ on the spontaneous Ca^{2+} transients between electrical stimuli. **A.** Representative images showing the fluo-4 fluorescence in the pulmonary vein between electrical stimuli (top panels) and during an electrical pulse (bottom panels), when the $[Ca^{2+}]_o$ was 2.5 mM (left panels) and 4.5 mM (right panels). Scale bar = 20 μm. **B.** Representative recordings displaying the fluo-4 fluorescence during EFS at 1 Hz in individual cardiomyocytes using ROI analysis, in a control recording and after increasing the

$[Ca^{2+}]_o$ to 4.5 mM. Spontaneous Ca^{2+} transients are indicated by asterisks. **C.** Mean frequency of spontaneous Ca^{2+} transients, between those that were evoked, in the control recordings and after increasing the $[Ca^{2+}]_o$. $P<0.001$ determined by Student's paired t-test and n = 16 cardiomyocytes (7 PVs from 6 rats).

Figure 6. Spontaneous Ca^{2+} transients in the rat pulmonary vein after a 5 s period of EFS. **A.** Wide-field image depicting the ROI that was used to produce the representative recordings of fluo-4 fluorescence during a control recording and after a short period of EFS at varying frequencies (1-9 Hz). The fluorescence across the dashed white line was used to produce the pseudo-linescan images. Representative recordings were obtained after increasing $[Ca^{2+}]_o$ to 4.5 mM. Scale bar represents 20 μm. **B.** Frequency, **C.** amplitude and **D.** velocity, following EFS at 1-9 Hz under in standard PSS and after increasing $[Ca^{2+}]_o$. $^{*}P<0.05$, $^{***}P<0.001$ *vs.* Cont. (No prior EFS) determined with repeated measures ANOVA with Dunnett's multiple comparison test. In standard PSS, n = 26 cardiomyocytes (6 PVs from 6 rats) for the amplitude and frequency, and 21 cardiomyocytes (7 PVs from 7 rats) for wave velocity. After increasing $[Ca^{2+}]_o$, n = 34 cardiomyocytes (6 PVs from 6 rats) for amplitude and frequency, and 32 cardiomyocytes (6 PVs from 6 rats) for wave velocity.

Figure 7. Synchronisation of spontaneous Ca^{2+} transients in the rat pulmonary vein after a short period of EFS. **A.** Representative analysis of spontaneous Ca^{2+} transient synchronisation in a control recording without prior EFS, and immediately following a period of EFS at varying frequencies (1-9 Hz). Representative recordings were obtained after increasing $[Ca^{2+}]_o$ to 4.5 mM. The wide-field images are threshold images, displaying pixels that have an intensity greater than their half-maximal intensity during the recording as white, and pixels with a lower intensity as black. The ROI used for the analysis is shown in the top

left panel. The recordings to the right represent the synchronisation index for each frame over time under conditions where there was no prior EFS (black), and after a period of EFS at 1-9 Hz (blue). Scale bar represents 10 μm. **B.** The maximum synchronisation index in standard PSS during the first 2 s and last 2 s of the recording period with no prior EFS, and immediately following a period of EFS at 1-9 Hz. Data represent mean ± s.e.m and n = 6 PVs from 6 rats. **C.** The maximum synchronisation index in high $[Ca^{2+}]_o$, during the first 2 s and last 2 s of the recording period, with no prior EFS and immediately following a period of EFS at 1-9 Hz. Date represent mean ± s.e.m. $^{*}P<0.05$ and $^{**}P<0.01$ *vs.* Cont. (no prior EFS) determined with repeated measures ANOVA and Dunnett's multiple comparison test. n = 6 PVs from 6 rats.

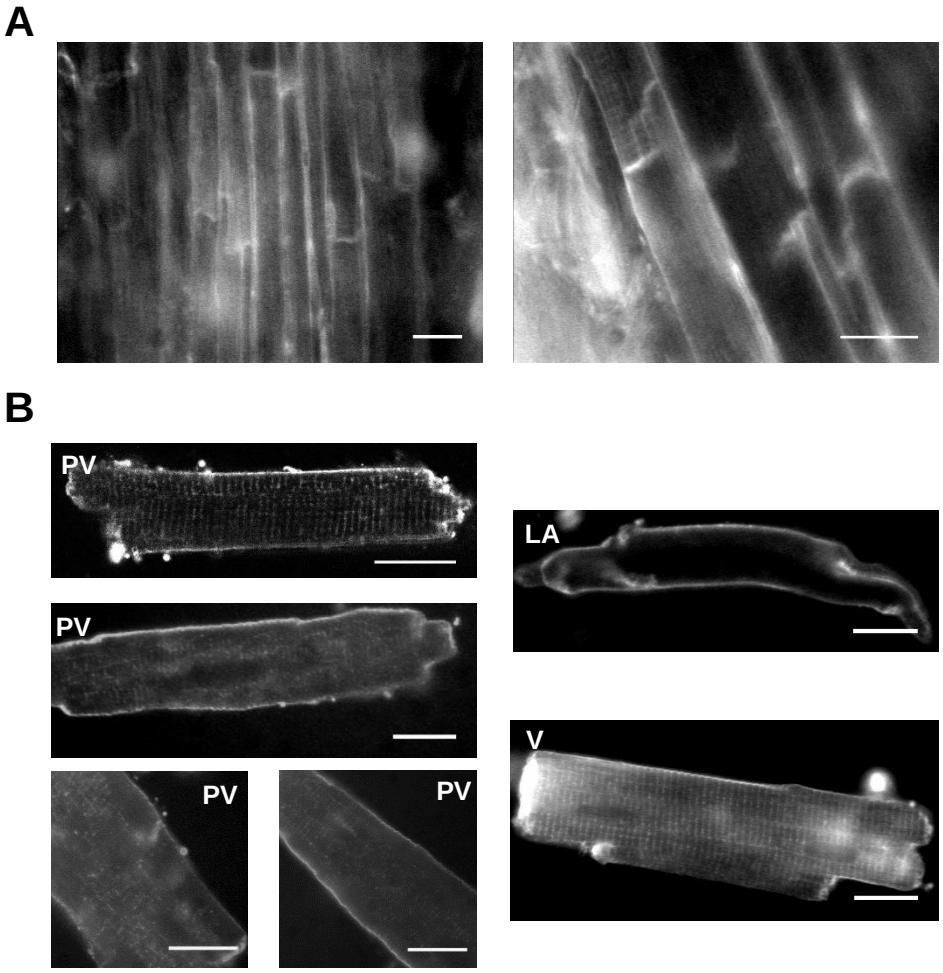
A
B
PV
PV
PV
PV
LA
V
C
Length (µm)
200
150
100
50
0
***
###
PV
LA
V
Width (µm)
50
40
30
20
10
0
‡‡‡
*
###
PV
LA
V

Figure 1

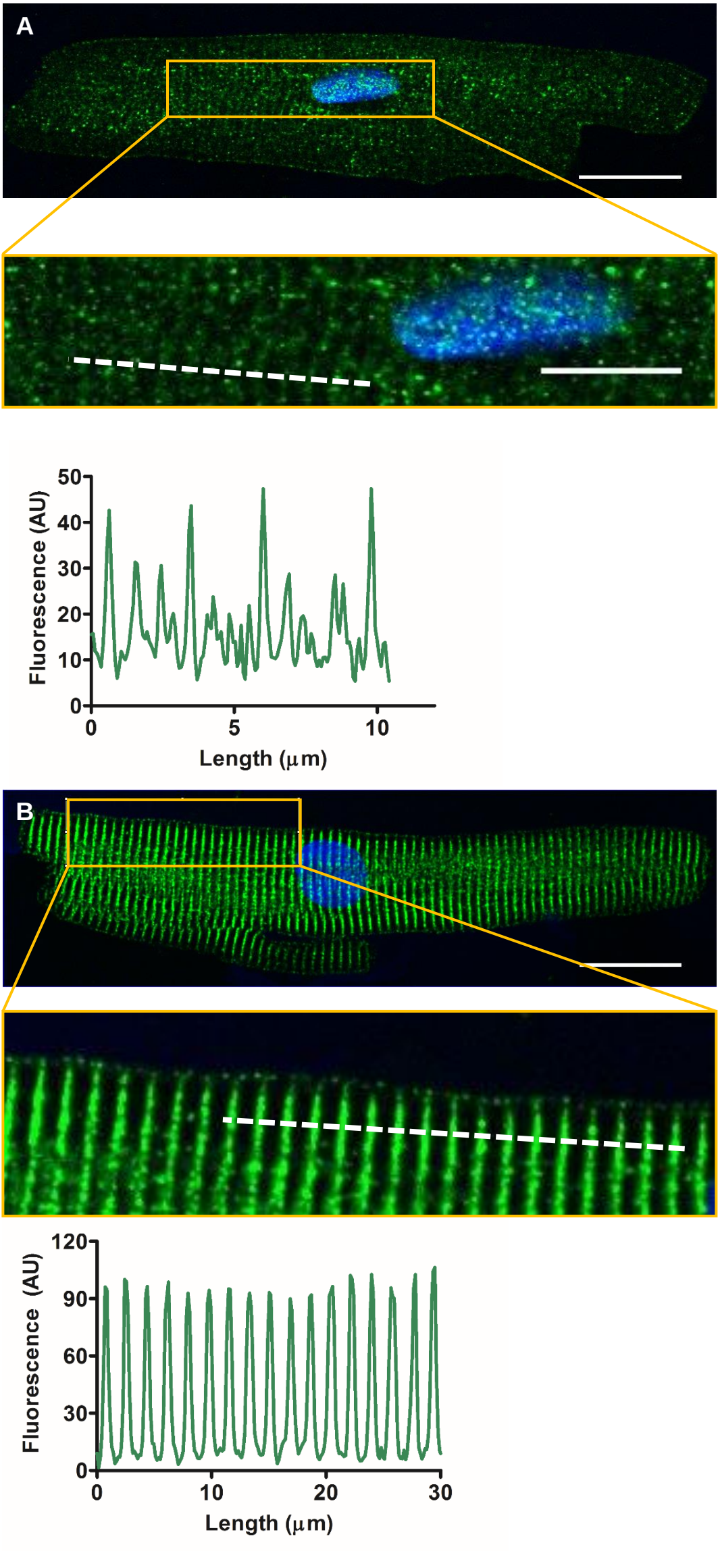
A
Fluorescence (AU)
50
40
30
20
10
0
0
5
10
Length (μm)
B
Fluorescence (AU)
120
90
60
30
0
0
10
20
30
Length (μm)

Figure 2

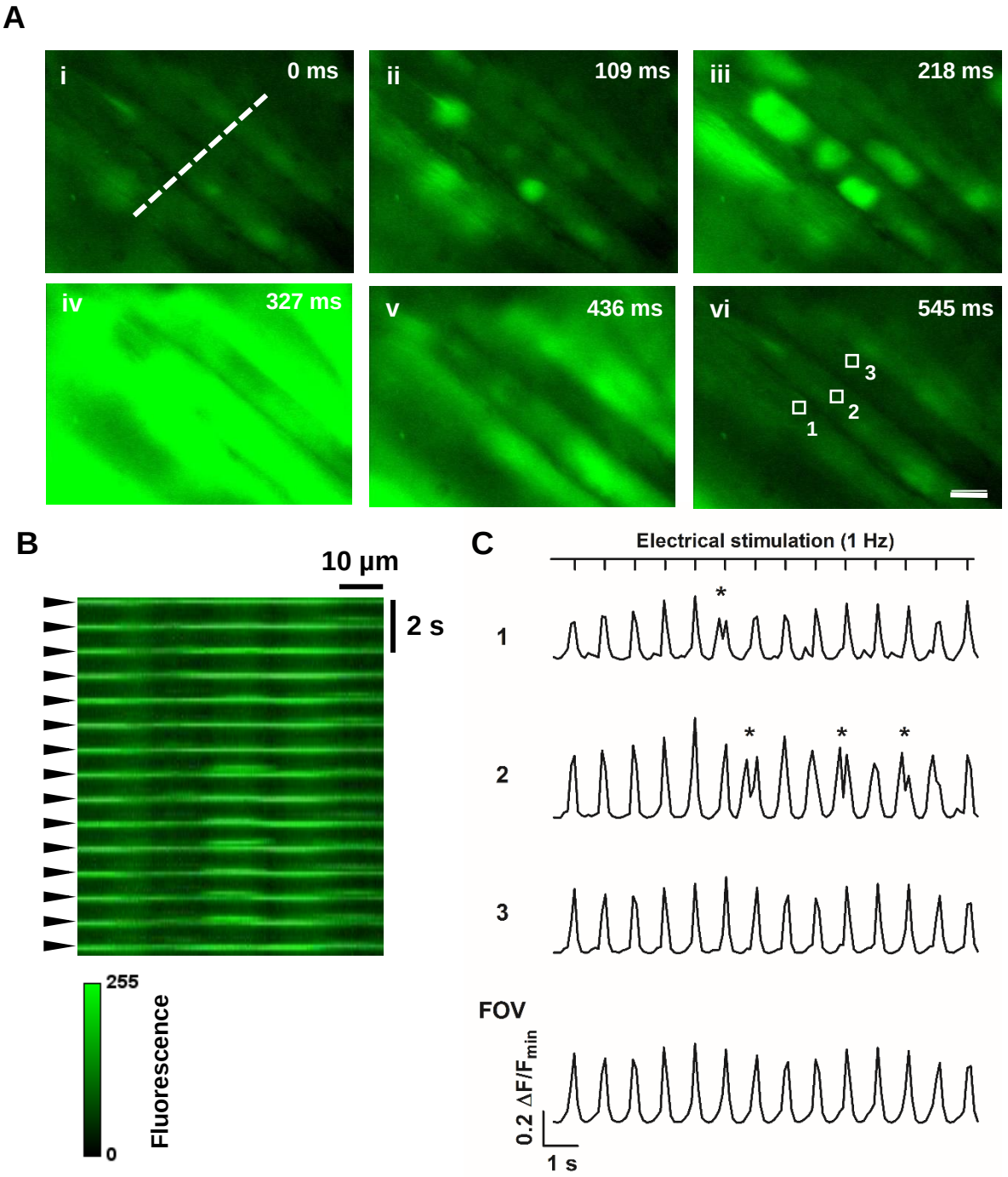
A
i
0 ms
ii
109 ms
iii
218 ms
iv
327 ms
v
436 ms
vi
545 ms
3
2
1
B
10 µm
2 s
255
0
Fluorescence
C
Electrical stimulation (1 Hz)
1
2
3
FOV
0.2 ΔF/F min
1 s

Figure 3

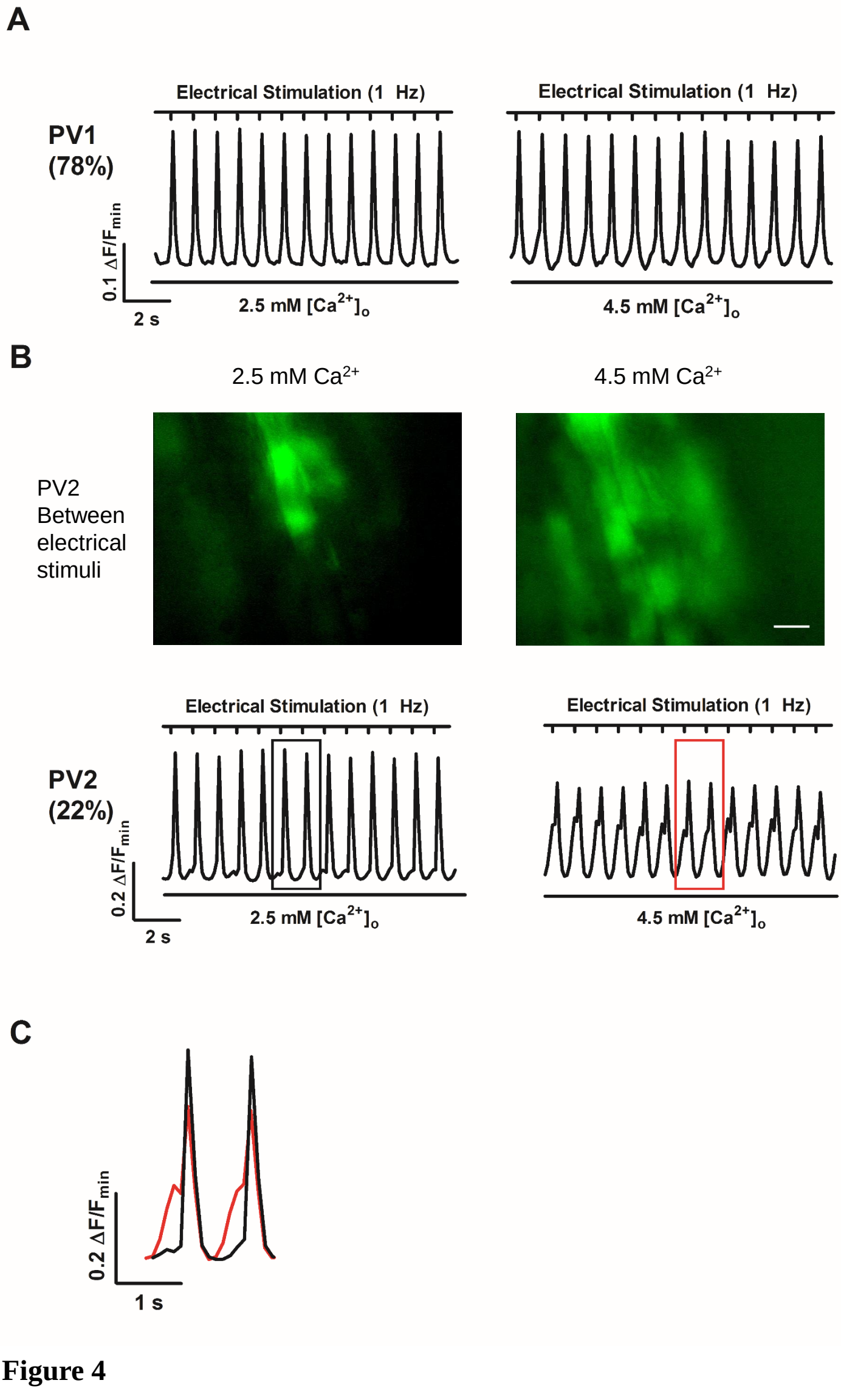
A
Electrical Stimulation (1 Hz)
Electrical Stimulation (1 Hz)
PV1
(78%)
0.1 ΔF/Fmin
2 s
2.5 mM [Ca2+]o
4.5 mM [Ca2+]o
B
2.5 mM Ca2+
4.5 mM Ca2+
PV2
Between
electrical
stimuli
Electrical Stimulation (1 Hz)
Electrical Stimulation (1 Hz)
PV2
(22%)
0.2 ΔF/Fmin
2 s
2.5 mM [Ca2+]o
4.5 mM [Ca2+]o
C
0.2 ΔF/Fmin
1 s

Figure 4

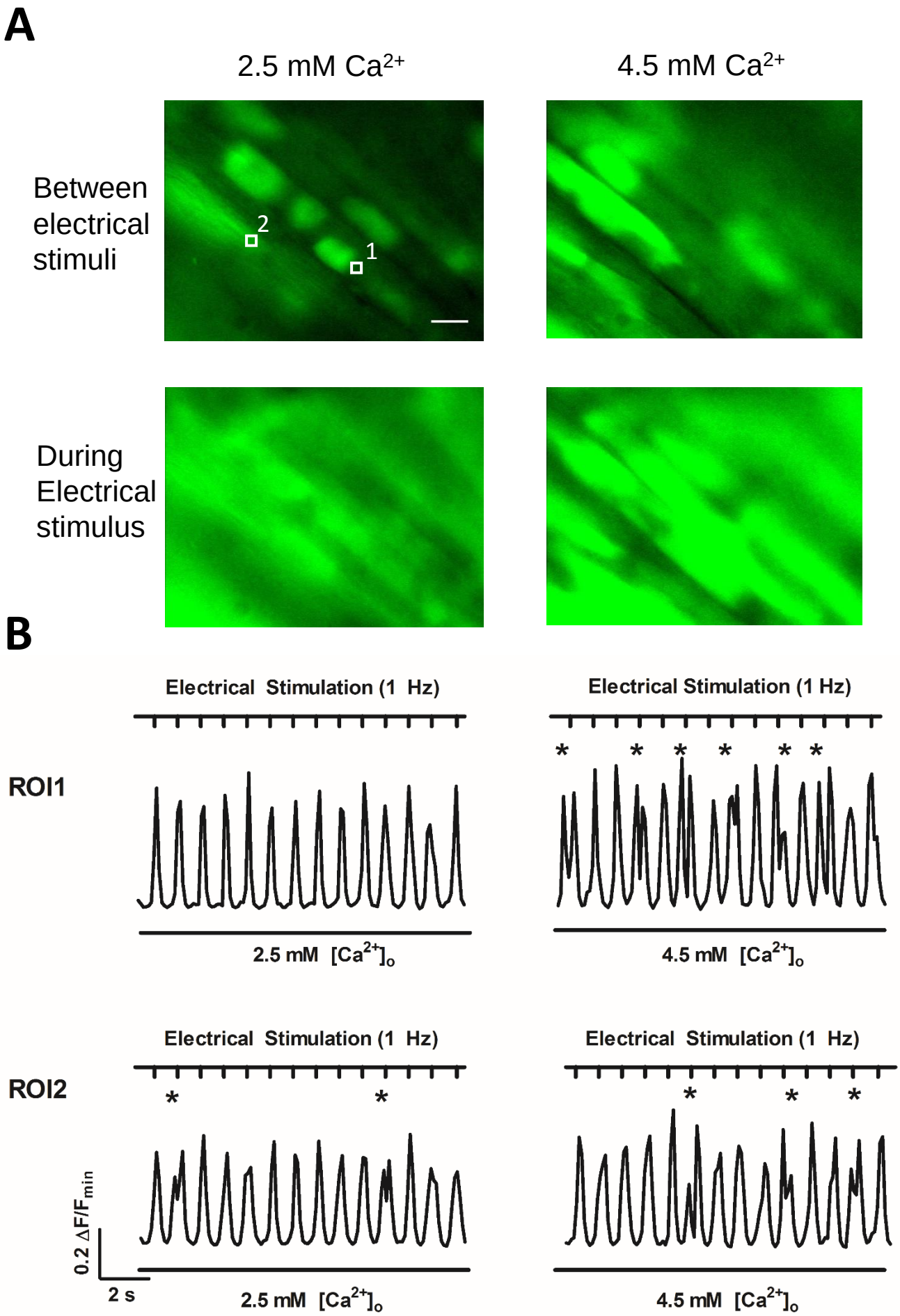
A
2.5 mM Ca2+
4.5 mM Ca2+
Between electrical stimuli
2
1
During Electrical stimulus
B
Electrical Stimulation (1 Hz)
ROI1
2.5 mM [Ca2+]o
Electrical Stimulation (1 Hz)
4.5 mM [Ca2+]o
ROI2
0.2 ΔF/Fmin
2 s
2.5 mM [Ca2+]o
4.5 mM [Ca2+]o
C
Frequency (Hz)
0.5
0.4
0.3
0.2
0.1
0.0
***
2.5 mM
4.5 mM
[Ca2+]o

Figure 5

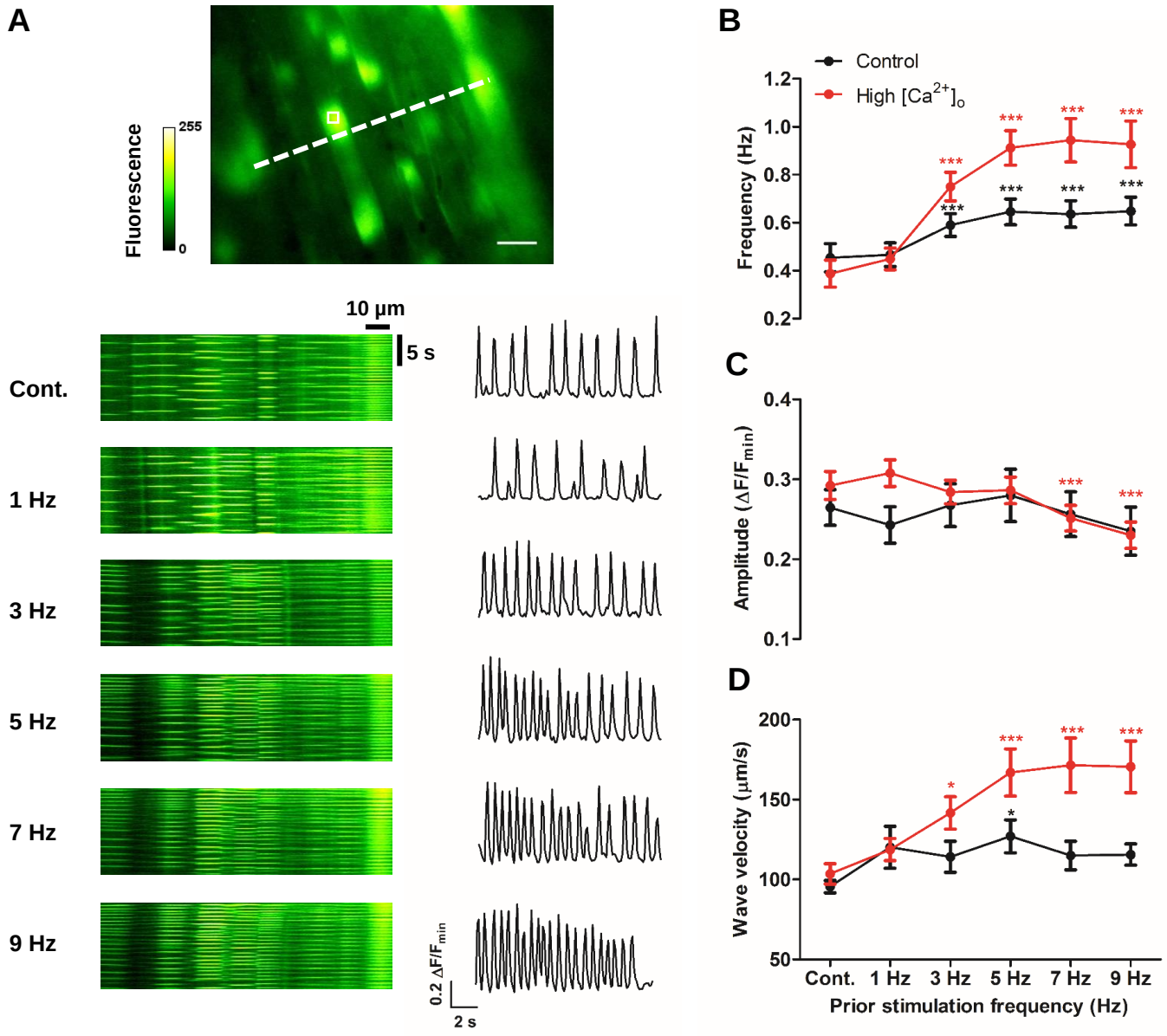
A
Fluorescence
255
0
10 µm
5 s
Cont.
1 Hz
3 Hz
5 Hz
7 Hz
9 Hz
0.2 ΔF/F$_{min}$
2 s
B
Control
High [Ca^{2+}]$_o$
Frequency (Hz)
1.2
1.0
0.8
0.6
0.4
0.2
C
Amplitude (ΔF/F$_{min}$)
0.4
0.3
0.2
0.1
D
Wave velocity (µm/s)
200
150
100
50
Cont.
1 Hz
3 Hz
5 Hz
7 Hz
9 Hz
Prior stimulation frequency (Hz)

Figure 6

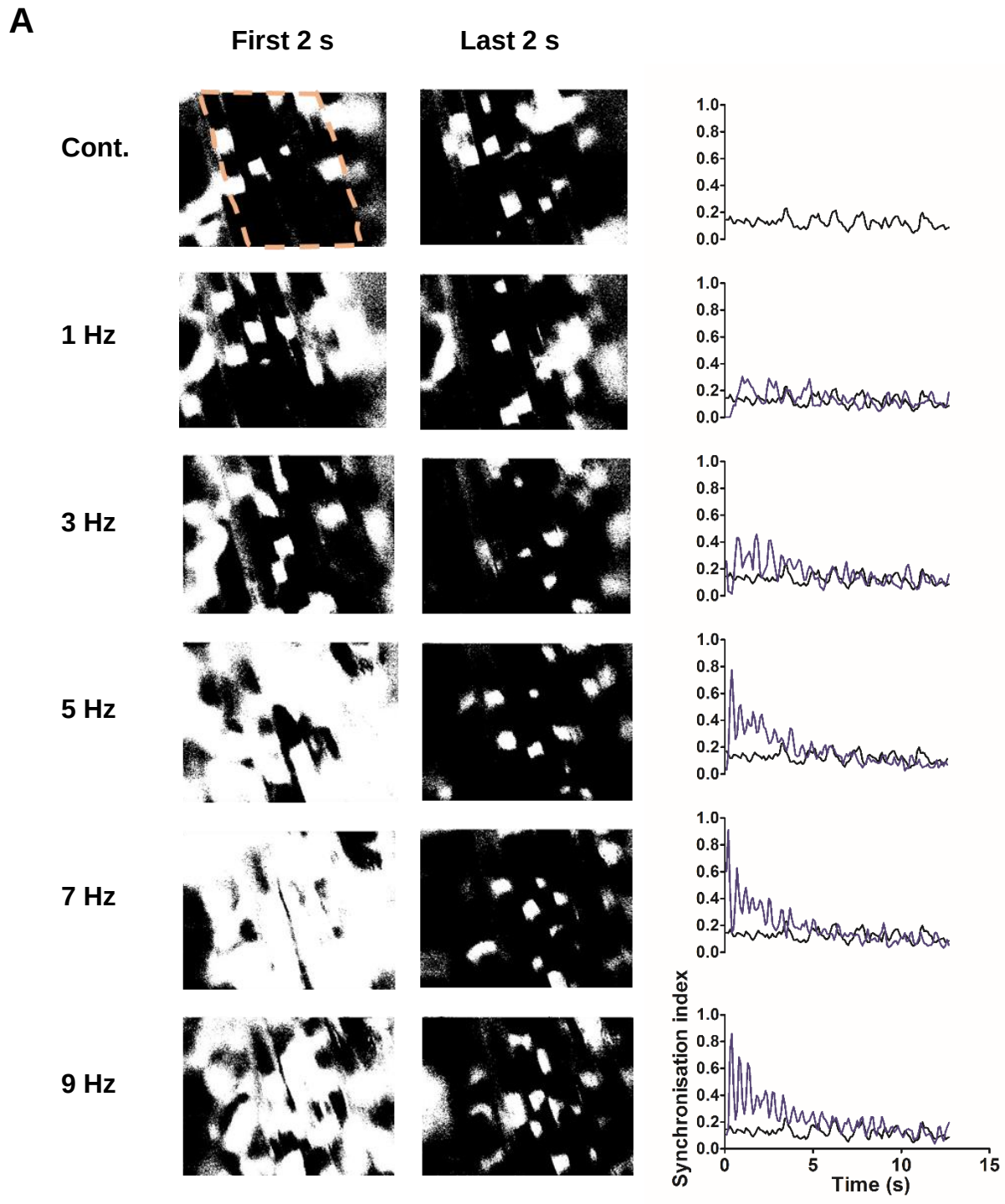
A
First 2 s
Last 2 s
Cont.
1 Hz
3 Hz
5 Hz
7 Hz
9 Hz
Synchronisation index
Time (s)
B
Control
C
High [Ca2+]o
First 2 s
Last 2 s
Max synchronisation index
Cont. 1 Hz 3 Hz 5 Hz 7 Hz 9 Hz
Prior stimulation frequency (Hz)
**
**
*

Figure 7